ICAS 2021 SHANGHAI
International Council of the Aeronautical Sciences
32nd Congress of the International Council of the Aeronautical Sciences
September 6-10, 2021 Pudong Shangri-La, Shanghai, China

AERODYNAMICS DESIGN, OPTIMIZATION AND FLOW FIELD INVESTIGATION OF A CONTRA-ROTATING PROPFAN AT HIGH FLIGHT MACH NUMBERS

Tao Wu, Zhida Li, Wei Dong

School of Mechanical Engineering, Shanghai Jiao Tong University, Shanghai 200240, China

Tel: 086-021-34204410; Fax: 086-021-62932242;

Email: wdong@sjtu.edu.cn

Abstract

Open-rotor engine, due to its ultra-high bypass ratio, can maintain relatively high propulsion efficiency and enable large reductions in fuel burn at Mach number around 0.8. Now, major aero engine manufacturers have resumed the development of counter-rotating open rotor engines. While, with respect to the design of counter-rotating propeller, no conclusion has yet been reached on whether external flow design method of propeller or internal flow design method of compressor is more suitable. In the paper, the design of counter-rotating propeller was carried out with internal flow design method and the interaction between front and rear blades were investigated, which is of great importance to the design of counter-rotating propeller.

In order to reduce the blade loading and noise, a blade count configuration of 12x10 was chosen in the paper. After giving the initial design thrust value of the front and rear blade, the distribution of the airflow parameters along the spanwise location under radial equilibrium was calculated and given as the initial value for geometry modeling. Then the parametric blade modeling tool is used to complete the three-dimensional modeling of the blade and the preliminary design of the front blade is completed. In the geometric modeling process, the initial blade geometry was obtained by using the Winnerstrom thickness distribution for the design of high load axial compressor. After the preliminary design of the front blade is completed, according to the CFD simulation results, the front blade is optimized by adjusting the geometric parameters and flow parameters of the blade. Using the flow parameters of the front blade, the aerodynamic design and three-dimensional modeling of the whole propeller fan are completed by the method of three-dimensional iterative optimization design. The design result reaches the design standard. At the same time, the characteristics of the flow field of the designed contra rotating propellers are also studied.

Keywords: Contra rotating propellers Aerodynamic design Optimization design Flow field simulation

1. Introduction

The open-rotor engine is also known as the Propfan engine, also known as the Unducted fan engine, the concept was first put forward by the National Aeronautics and Space Administration in the 1970s[1]，Therefore, the open-rotor engine can be regarded as either a turboprop engine with advanced high-speed propellers or a turbofan engine with a high bypass ratio without outer passages. In recent years, more and more attention has been paid to the counter-rotation technology as one of the effective techniques to improve the thrust-weight ratio of aeroengines and aircraft performance [2]. Since the last century, with the development of aerodynamic thermodynamics and computational fluid mechanics, the design system of axial flow compressor has been continuously improved, leading to the improvement of compressor design level. To meet the basic requirements of high performance aero-engine compressor is small size, light weight, good performance, safety and reliability [3-4]. The quasi-three-dimensional design system is developed from the theory of two types of relative flow surfaces (S1 flow surface and S2 flow surface) proposed by Wu Chung-Hua in 1952[4] ，

Streamline curvature method [4-7] was first proposed to solve the steady axisymmetric flow in turbomachinery. It is a method to solve the equation of motion and continuity equation along each given calculation station. This method avoids the difficulty of numerical solution by considering only one major factor. In addition, according to the U.S. Advanced Turbine Program (ATP), the advanced open-rotor engine can maintain a relatively low fuel consumption rate at an altitude of 1067 *m,* around *Ma*0.8, compared to conventional turboprop engines [8] Therefore, it is of great significance to carry out the research on the reverse rotation technology. As early as 1913, Ljungstrom in the United States made the first runoff reverse turbine, but it did not arouse the attention of the world aviation community. Then, it was not until 1957 that the aerodynamic efficiency analysis of two-stage axial-flow contra-rotating turbines was carried out [9]. Although in 1954, the British Rolls-Royce [10] engine proposed the original scheme, is the use of two rotor relative to the opposite rotation of the dual rotor scheme.

in this paper, three-dimensional bade modeling software [11] is used to conduct three-dimensional modeling of the blade. The modeling software has a professional blade modeling module, and the modeling program of all aspects of the blade refers to the program used by Dr. Ali Merchant [12-16]. After the blade modeling was completed, the three-dimensional modeling of the blade was optimized by adjusting the geometric and aerodynamic parameters of the blade according to the CFD simulation results. The three-dimensional iterative optimization method was used to complete the whole blade modeling. Finally, the flow field characteristics of the contra-rotating propellers are studied by numerical simulation.

2. Design indicators

The design parameters of this paper refer to Table 1:

Tabla1 Initial design parameters of the contra-rotating propellers

Environmental conditions	Flight altitude(m)	10668
	Flight Mach number	0.785
Front blade	Hub ratio	0.42
	Rotating speed (rpm)	1000
	Tip diameter (m)	4.5
	Number of blades	12
	Thrust (N)	13000
Rear blade	Hub ratio	0.42
	Rotating speed (rpm)	1000
	Tip diameter (m)	4.5
	Number of blades	10
	Thrust (N)	12000

3. Preliminary design and optimization

3.1 Blade molding method

The modeling module of modeling [11] software is used for three-dimensional blade modeling in this paper, and the specific process is shown in Fig.1. The input file [11] is a code for three-dimensional blade modeling, which contains the aerodynamic parameters and geometric parameters needed to define and construct three-dimensional blade shapes.

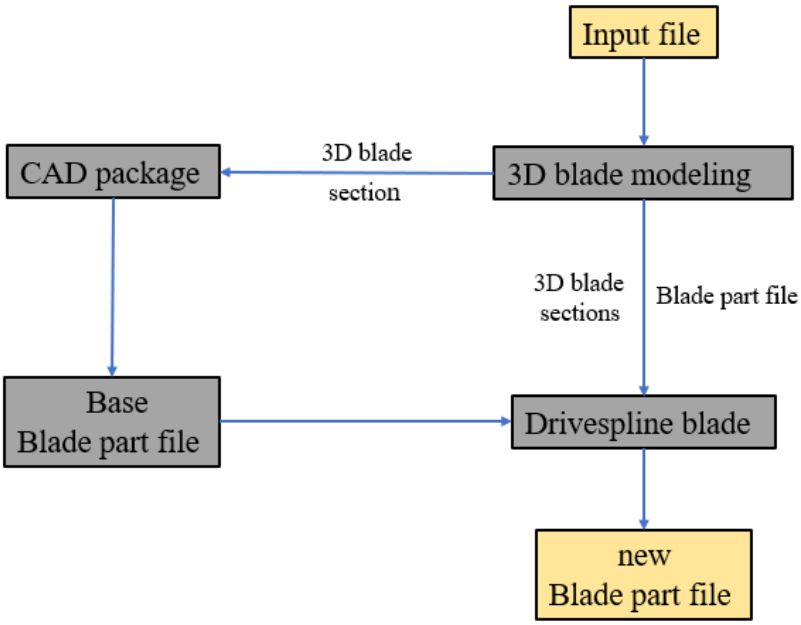

Figure 1 – Flow chart of blade design

The parameters of each streamline passing through the blade are defined as follows:

1. Flow Angle of leading edge and trailing edge of blade.
2. Relative inlet Mach number.
3. Ratio of blade thickness to chord length.
4. Axial chord length value.
5. Attack angle and deviation angle (if equal to zero, flow angle represents blade geometric angle).

3.2 Distribution of initial blade geometrical parameters

The change of axial velocity was estimated by using the thrust of the front blade, and then the distribution of the initial flow parameters and geometric parameters of the front blade was obtained by using the velocity triangle and combining with the parameters given in Table 1, which were used as the input parameters of the blade modeling software. The distribution of inlet and outlet geometric angles of the initial blade profile is given, as shown in Fig. 2.

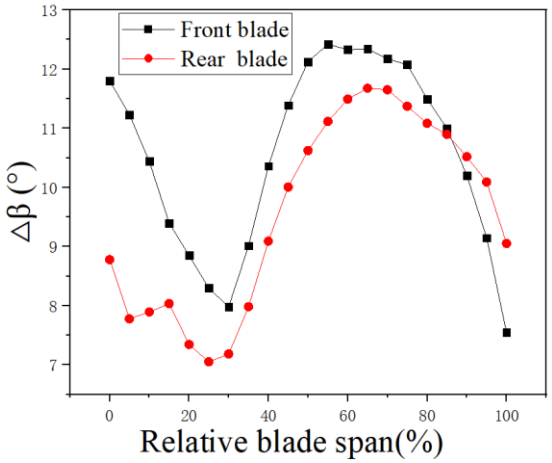

Figure 2 – Distribution of inlet and outlet geometrical angles of initial blade profile

Firstly, the relevant parameters of the front blade were designed, and the blade geometry was defined by 21 sectional geometrical parameters at different height of the blade. Blade modeling is based on the assumption that airflow moves along the flow surface of a cylinder. Because of the assumption that airflow moves along the flow surface of a cylinder, it is convenient to calculate the variation of airflow parameters before and after the blade and the three-dimensional modeling, so the streamline coordinates can be conveniently given. In addition, the maximum thickness to chord length ratio, the

pitch axis, and the distribution of airflow deflection angle are given in the corresponding three-dimensional modeling according to the relevant input in the references [17]. The preliminary distribution of front blade shape design and relevant data are shown in Fig. 3. Therefore, the required inputs of the 3D blade modeling software have been given, and the geometric modeling of the initial blade profile can be completed.

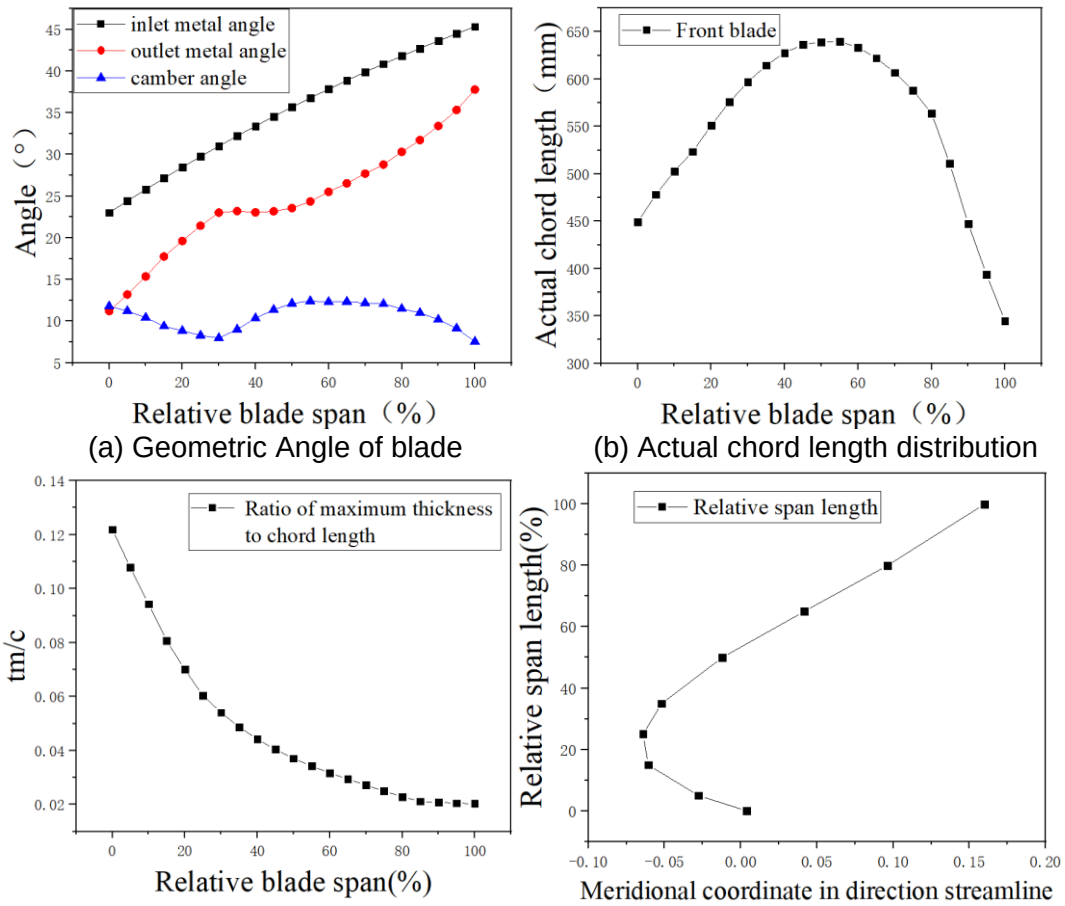

(a) Geometric Angle of blade (b) Actual chord length distribution

(c) Maximum thickness to chord length ratio (d) Distribution of front blade span

Figure 3 – Geometric parameter distribution of front blade

3.3 Description of blade thickness distribution

The blade thickness calculation method in this paper adopts a dimensionless thickness calculation method published by scholar Wennerstrom[18], in which the parameters are defined as shown in Fig. 4:.

1. x = Dimensionless mean camber line
2. x_T = Position of maximum airfoil thickness
3. t_1 = Thickness of blade leading edge
4. T = Maximum airfoil thickness.
5. t_2 = Thickness of blade trailing edge.
6. y_1 = Thickness of the upper half of the airfoil
7. y_2 = Thickness of the lower half of the airfoil.

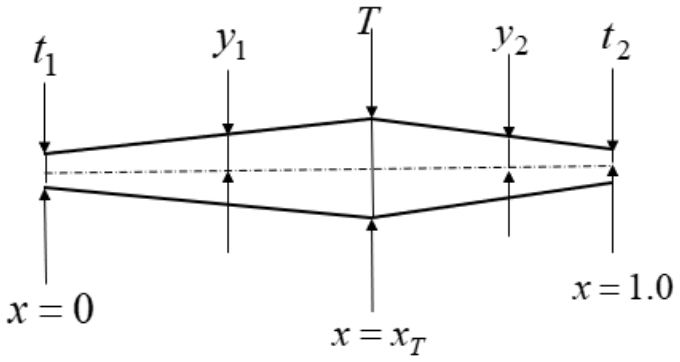

Figure 4 – Thickness distribution over mean camber line length in dimensionless

The calculation formula of blade thickness can be obtained as follows:

Thickness formula at $x < x_T$

$$y_1 = ax^3 + bx^2 + cx + d \quad (1)$$

$$y_1' = 3ax^2 + 2bx + c \quad (2)$$

$$y_1' = 3ax^2 + 2bx + c \quad (3)$$

$$y_1'' = 6ax + 2b \quad (4)$$

Thickness formula at $x > x_T$：

$$y_2 = e(x - x_T)^3 + f(x - x_T)^2 + g(x - x_T) + h \quad (5)$$

$$y_2' = 3c(x - x_T)^2 + 2f(x - x_T) + g \quad (6)$$

$$y_2'' = 6c(x - x_T) + 2f \quad (7)$$

When $x_T > 0.5$， the boundary condition：

$x = 0$

$$y = \frac{t_1}{2} \quad (8)$$

$$y_1'' = 0 \quad (9)$$

$x = x_T$

$$y_1 = y_2 = \frac{T}{2} \quad (10)$$

$$y_1' = y_2' = 0 \quad (11)$$

$$y_1'' = y_2'' \quad (12)$$

$$y_2 = \frac{t_2}{2} \quad (13)$$

According to the above formula, the distribution of blade thickness of the propeller fan can be calculated. The coefficients from *a* to *h* are shown in Reference [18], which will not be explained in detail here. In addition, when $x_T < 0.5$， the correlation coefficient can be obtained by inverting the boundary conditions of leading edge and trailing edge.

3.4 Numerical analysis

The CFD analysis of the initial blade shape of the front blade was carried out, as shown in Fig. 5. For the calculation domain of the front blade, the distance between the front and rear was extended by 10 times the height of the propeller fan, and the range of the far-field height was set by 5 times

the height of the propeller fan. The surrounding boundary adopts the far-field boundary condition, and the incoming flow parameters are given in Table 1. *S-A* turbulence model is used for turbulence model and ideal gas is used for numerical calculation.

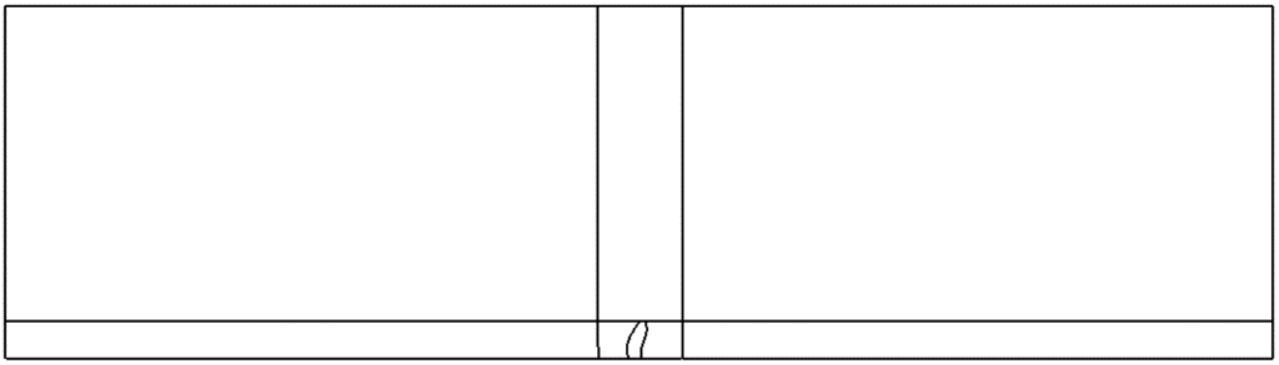

Figure 5 – Calculation domain of initial front blade profile

For the initial blade profile, static pressure, static temperature and total temperature increase in the area behind the front blade as shown in Fig. 6. As can be seen from Fig. 7, the static pressure ratio and total pressure ratio of front row of the contra rotating propellers are low.

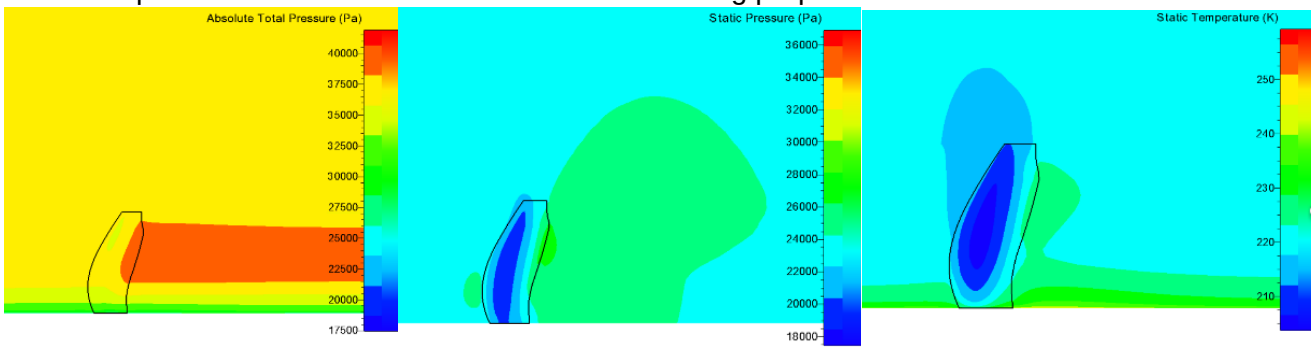

(a) Total pressure (b) Static pressure (c) Static temperature

Figure 6 – Distribution of flow parameters on the meridional view initial blade profile

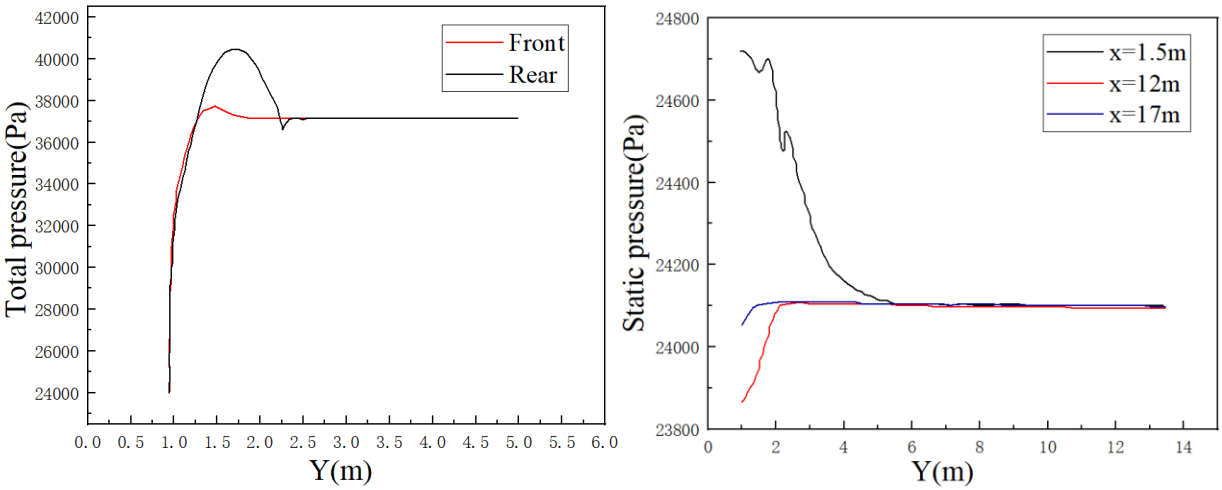

(a) Total pressure distribution along blade span (b) Static pressure distribution along blade span

Figure 7 – Distribution of total pressure and static pressure before and after paddle fan

As shown in Fig. 8, the axial velocity of the single row propeller fan increases to a certain extent after the propeller fan, but decreases to a certain extent outside the diameter of the propeller fan, which is in good agreement with the theoretical calculation results. As shown in Fig. 9, According to the static pressure curve the static pressure on the blade surface is close to or even opposite in some areas between the blade pressure surface and the suction surface, it indicates that the blade has weak power capacity and there is still much room for improvement in the design of the initial blade profile.

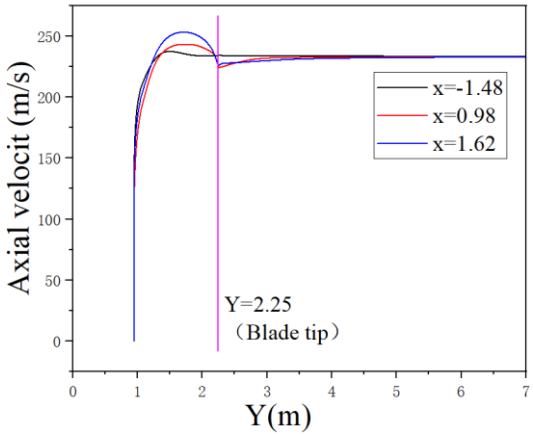

Figure 8 – Distribution of axial velocity

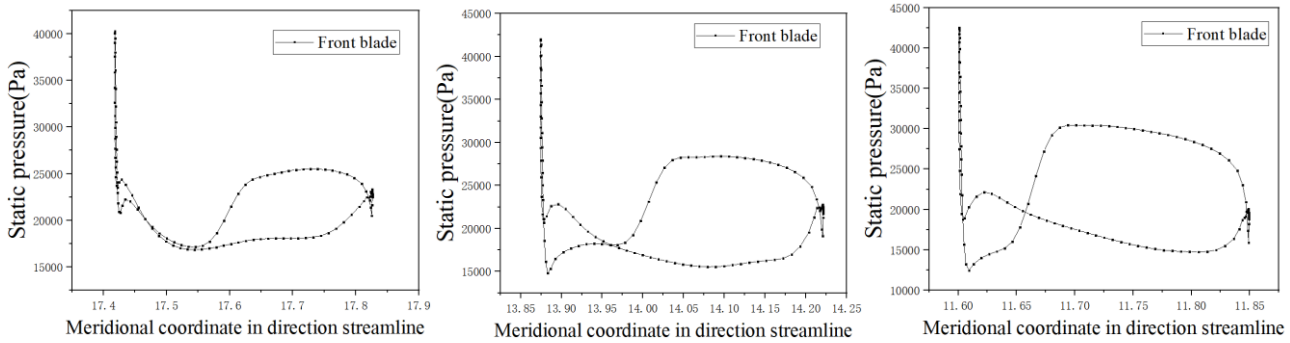

(a) 25% blade span (b) 50% blade span (c) 75% blade span

Figure 9 – Initial front blade profile static pressure distribution

Fig. 10 shows the relative Mach number distribution of blade height. An obvious shock wave structure appears at 30% blade height, and the airflow accelerates greatly on the suction surface and the relative Mach number of the airflow is large, resulting in large shock pressure loss. In addition, the research shows that the thrust value of the initial blade profile is 19570N (-X direction), the torque is 69188Nm, and the propulsion efficiency is 63%. Propulsion efficiency does not reach the design parameters. Therefore, further optimize and change its geometric parameters to improve its propulsion efficiency is needed.

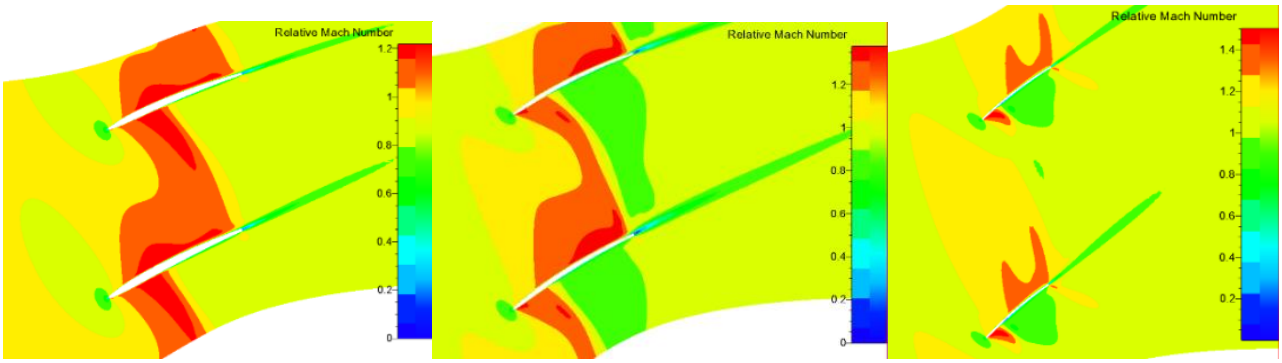

Figure 10 – Relative Mach number distribution of initial front blade

3.5 Optimization of geometric parameters

Because the propelling efficiency of the initial blade fan is relatively low, it is considered to optimize the design of the blade shape by modifying the geometric parameters, and to modify the initial blade profile to improve its propelling efficiency. As shown in Fig. 11, the preliminary optimization of the initial blade profile was completed by reducing the trailing edge radius, changing the position of the maximum thickness, and increasing/decreasing the leading edge inlet geometric angle.

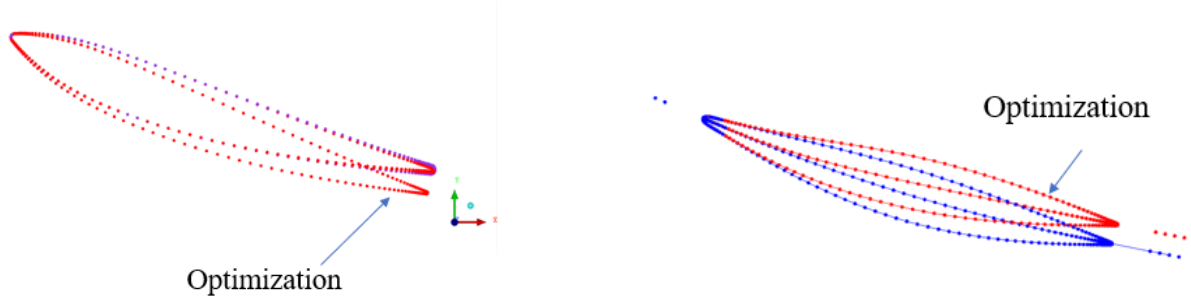

(a) Reduce the trailing edge radius (b) Change the mean camber line

Figure 11 – Modelling changes after changing geometric parameters

As shown in Fig. 12, after the modification of geometric parameters, the pressure distribution of different blade span was slightly improved, but the improvement of propulsion efficiency was still not significant. Therefore, simply changing the geometric parameters of three-dimensional modeling cannot significantly improve the propelling efficiency of the front blade, and it is necessary to change the pressure distribution at each blade span in order to improve the flow in the blade passage.

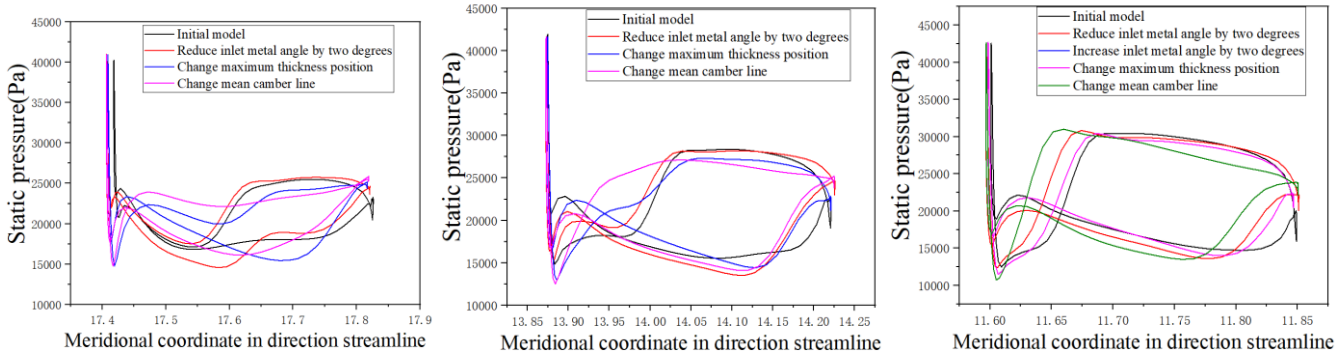

(a) 25% blade span (b) 50% blade span (c) 75% blade span

Figure 12 – Static pressure distribution of different front blade shapes

3.6 Optimization of flow parameters

The radial velocity is ignored and the airflow is assumed to flow along the cylinder surface. Based on the optimization design method proposed above, the propellant efficiency of the front blade does not reach the target. Therefore, it is necessary to carry out further iterative optimization design for a front blade. The flow parameters through each blade section are iterated with the three-dimensional calculation results, and the distribution of inlet metal angle and camber angle of each blade section is adjusted, and a certain distribution of attack angle is added to optimize the design. In this paper, an iterative optimization design of a front blade is carried out to obtain the modeling parameter distribution of the front blade.

After the initial blade profile is obtained, the airflow deflection angles of each blade section are iterated repeatedly to further improve the propulsion efficiency. After a certain iteration, the metal angle and camber angle distribution of each blade section of the front blade are shown in Fig. 13 (a). According to experience, a certain attack angle distribution was added to each blade section of the front blade to improve the flow condition of each blade height, as shown in Fig. 13 (b), and the distribution of other geometric parameters is shown in Fig. 14.

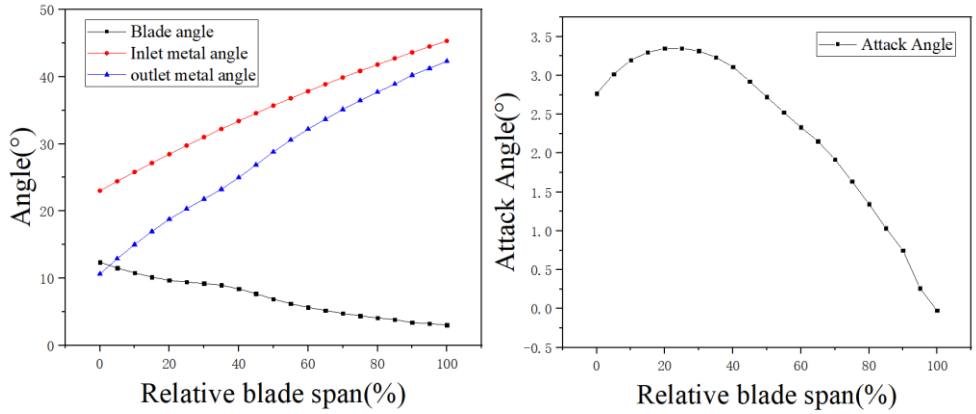

(a) Distribution of metal angle (b) Distribution of attack angle

Figure 13 – Geometric parameter distribution of the front blade after iterative optimization

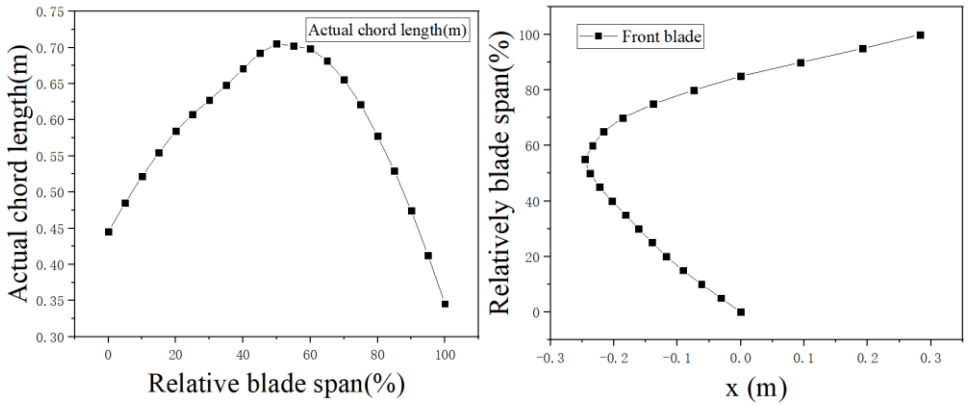

(a) Actual chord length distribution of front blade (b) Coordinate of the leading edge of the front blade (the hub of leading edge is the origin of X coordinate)

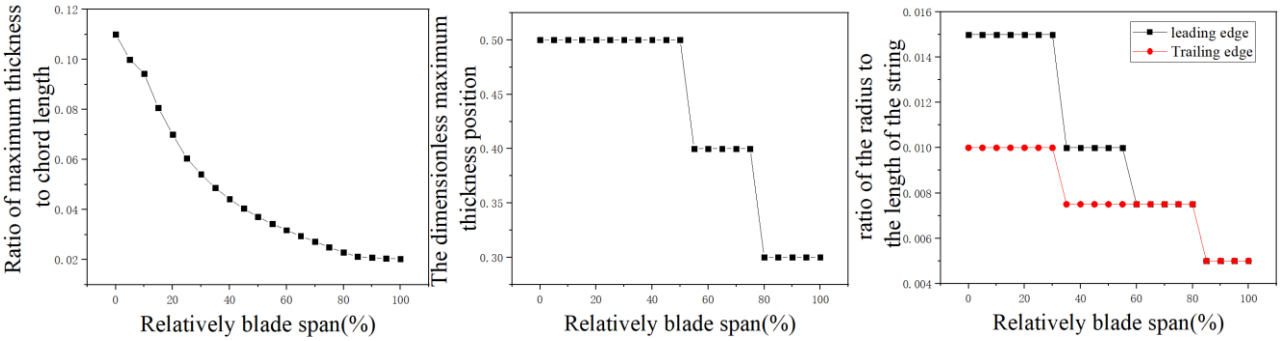

(c) Maximum thickness to chord length ratio (d) Position of maximum thickness (e) Leading and trailing edge radius

Figure 14 – Geometric parameter distribution of each blade height after iterative optimization

Table 2 shows the distribution of thrust and torque of the front blade after iterative optimization. Propulsion efficiency has been significantly improved, and the thrust value is also consistent with the expected design value. The research shows that the design of relevant parameters of the front blade of the propeller fan is reasonable.

Table 2 Distribution of thrust and torque of the front blade after iterative optimization

	Thrust (N)	Torque (Nm)	Propulsion efficiency (%)
Front blade	14809.96	43097.65	76.4

Flow characteristics of the front blade after iterative optimization are shown in Fig. 15. Compared with the initial blade profile, the relative Mach number of different blade section is significantly reduced, and the supersonic region is mostly concentrated in a small range of the leading edge of the blade, which significantly reduces the shock loss. At 90% of the blade height, the maximum relative Mach number is less than 1.3, which is controlled at a relatively low level.

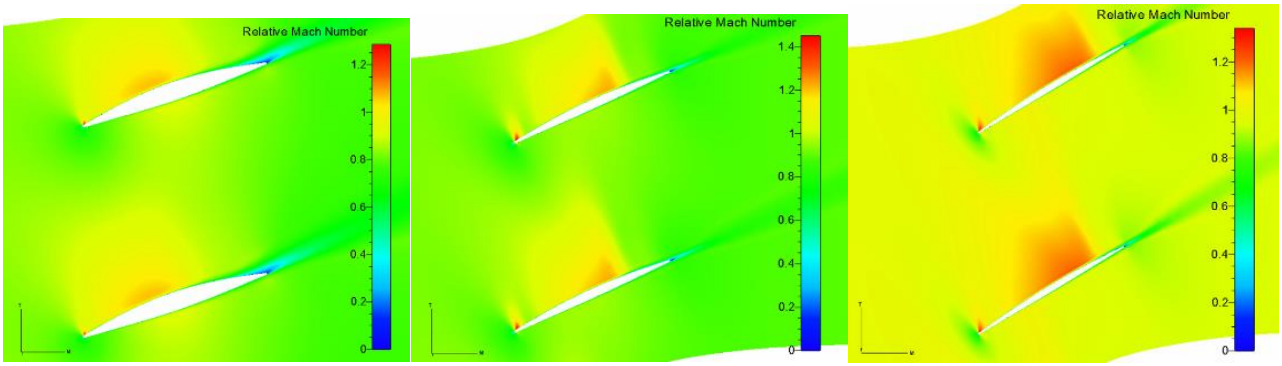

(a) 10% blade span (b) 30% blade span (c) 50% blade span

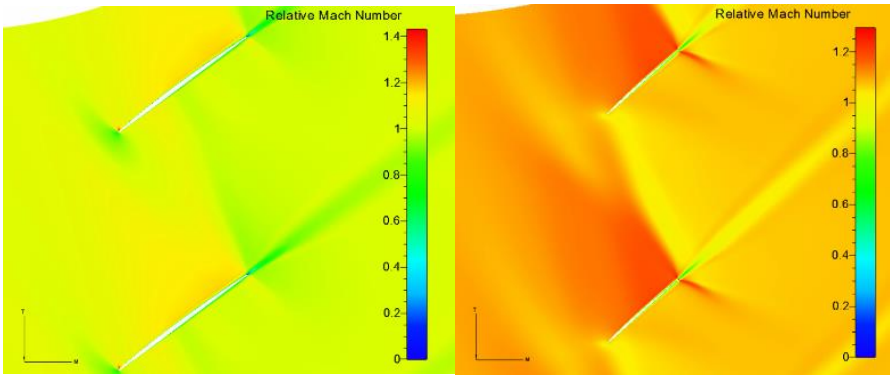

（d）70% blade span (e) 90% blade span

Figure 15 – Relative Mach number distribution of front blade

The static pressure distribution of each blade section in the front blade and the isentropic Mach number distribution on the blade surface are shown in Fig. 16, and the pressure distribution of each blade section have been significantly improved after iterative optimization. However, due to the blocking effect of the boundary layer at the blade root, the flow condition is not good.

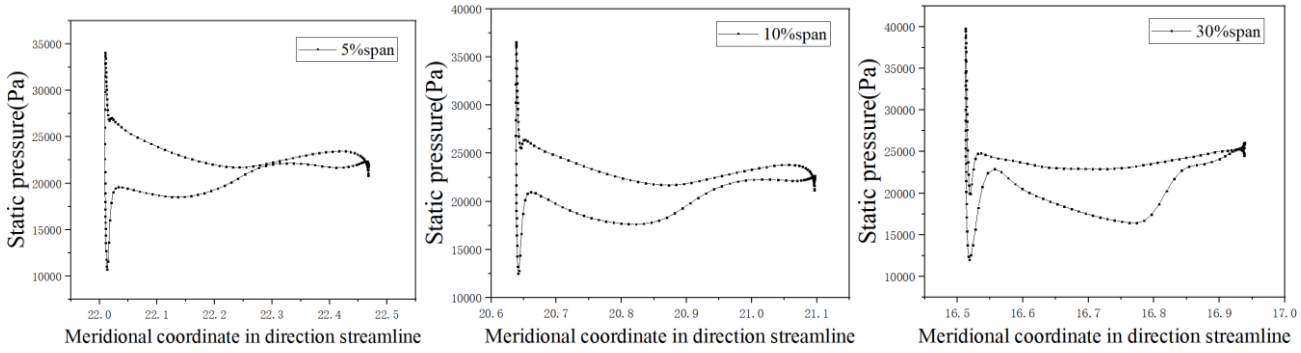

(a) 5% blade span (b) 10% blade span (c) 30% blade span

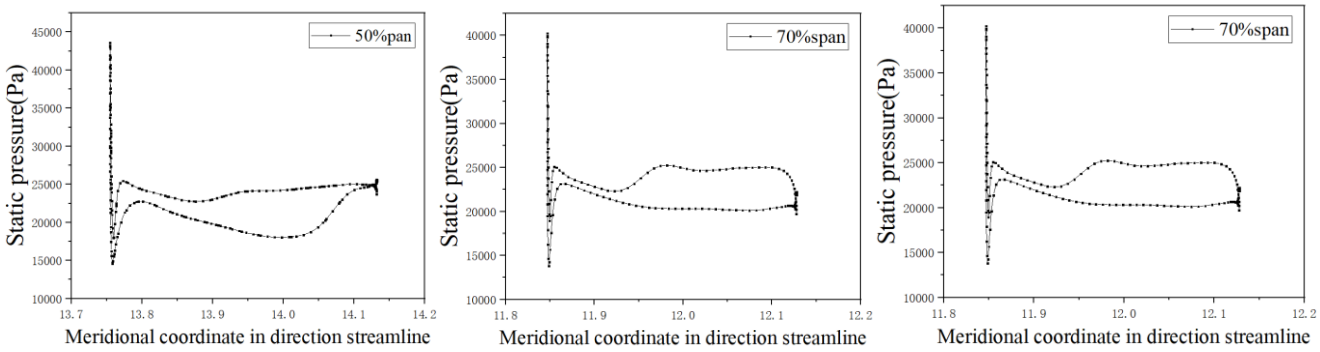

(d) 50% blade span (e) 70% blade span (f) 90% blade span

Figure 16 – Static pressure distribution of the front blade after iterative optimization

Fig. 17 shows the distribution of isentropic Mach number on the blade surface. There is no obvious over-acceleration region in the suction surface area of the blade, and the overall isentropic Mach number variation is controlled within a reasonable range.

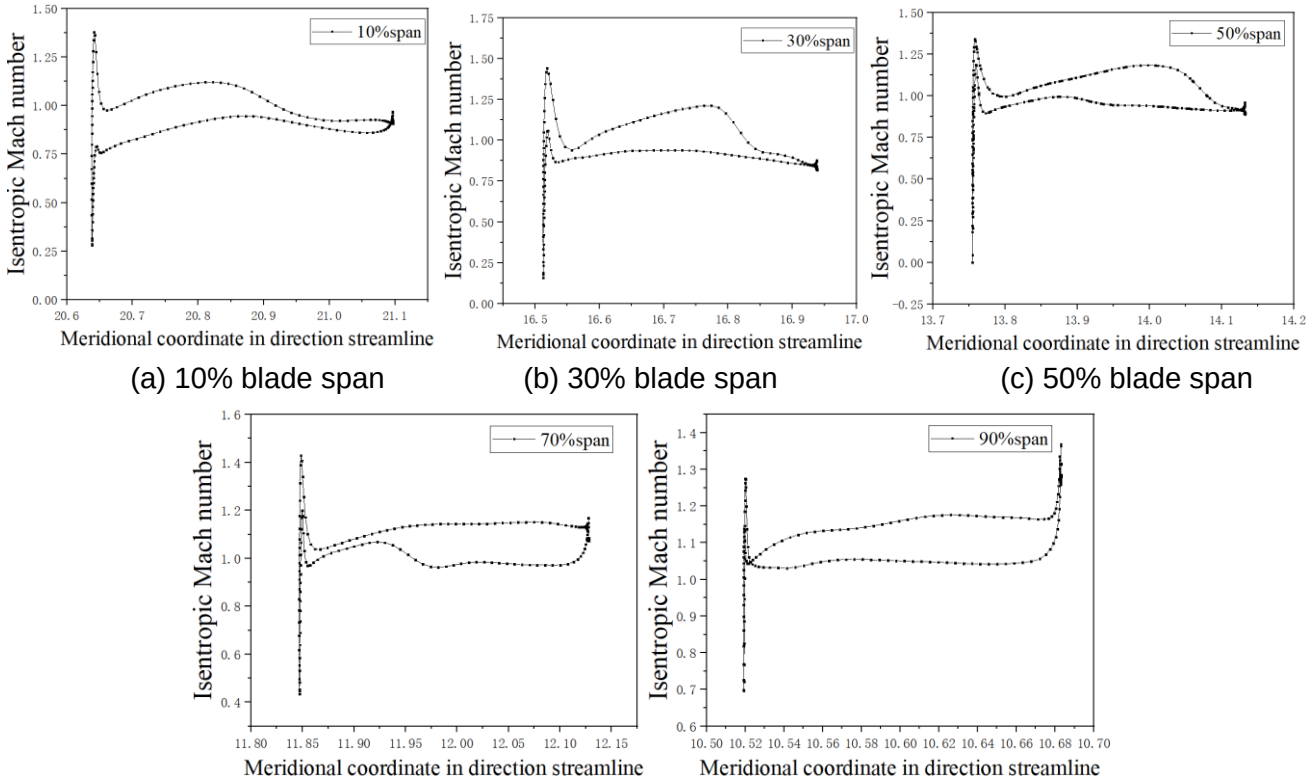

(a) 10% blade span (b) 30% blade span (c) 50% blade span

（d）70% blade span (e) 90% blade span

Figure 17 – Isentropic Mach number distribution on the front blade surface after iterative optimization

4. Flow characteristics of the optimized contra rotating propellers

According to the design and optimization results of the front blade, the flow parameters behind the front blade are obtained, which are used to carry out the preliminary design of the rear blade. Assuming that the rear blades axial outflow, the aerodynamic design and three-dimensional modeling of the front and rear rows of the contra rotating propellers were completed by using the three-dimensional iterative optimization design method. Fig. 18 shows the distribution of the coordinates of the leading edge points of the front and rear blades along the blade height. In order to reduce the noise generated during the operation of the contra rotating propellers, the front and back blades are designed with swept-back.

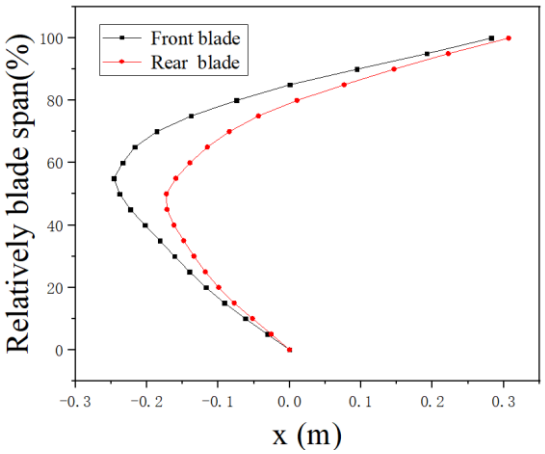

Figure 18 – Distribution of leading edge point coordinates of front and rear blades along blade span

The distribution of thrust, torque and propulsion efficiency are shown in Table 3. Based on the iterative optimization and Wennerstrom thickness distribution, the total propelling efficiency reaches 76.5%, which is in good agreement with the design parameters and basically meets the design requirements.

Table 3 Distribution of thrust and torque of the contra rotating propellers

	Thrust (N)	Torque (Nm)	Propulsion efficiency (%)
Front blade	14719.8	43281.7	75.65
Rear blade	14784.57	-42428.56	77.51
Paddle fan	29504.37	85710.26	76.57

Fig. 19 shows the relative Mach number distribution of the different span of the contra rotating propellers, and Fig. 20 shows the static pressure distribution on the blade surface. The shock wave mainly appears in the posterior area of the suction surface of the front blade and at the trailing edge of the rear blade. With the increase of the relative blade span, the shock wave moves more towards the trailing edge. In terms of static pressure distribution, the static pressure distribution of the front blade is basically the same as that of the front blade alone, and the influence of the rear blade on the flow of the front blade is small. After iterative optimization, although some areas in the front part of the rear blade did not play a good role in power generation, it had little influence on the design results. The design of the contra rotating propellers meets the design requirements.

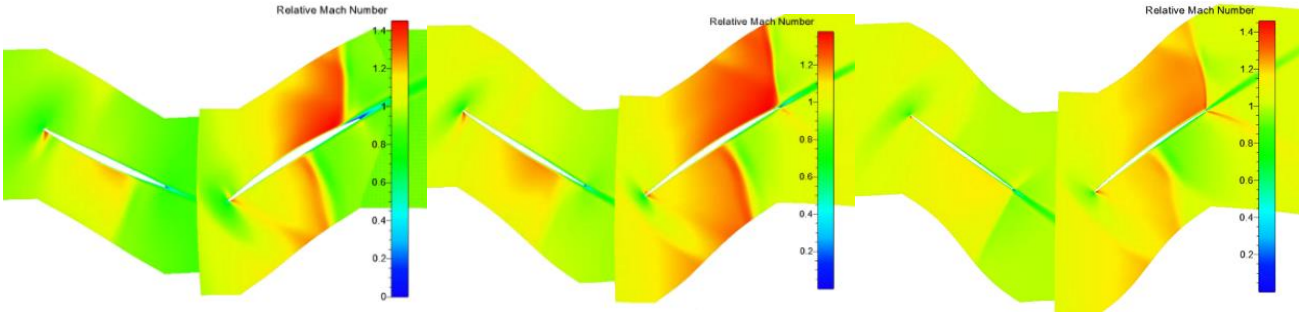

(a) 30% blade span (b) 50% blade span (c) 70% blade span

Figure 19 – Mach number distribution of the contra rotating propellers after optimization

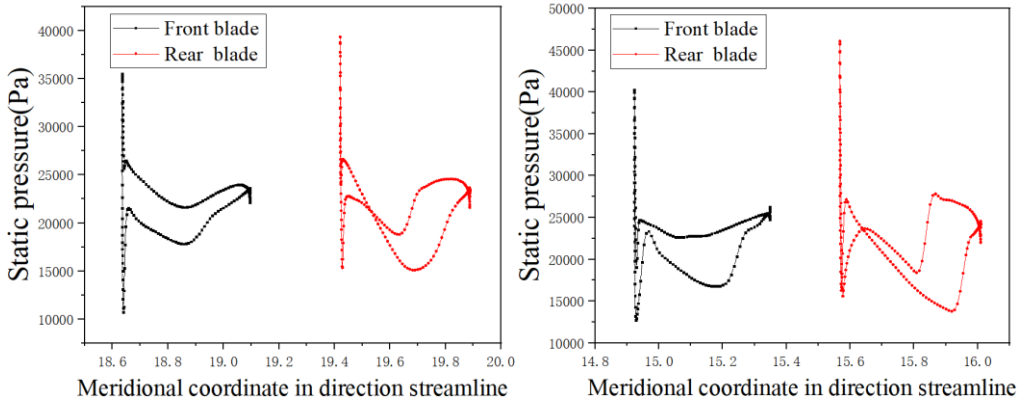

（a）10% blade span (b) 30% blade span

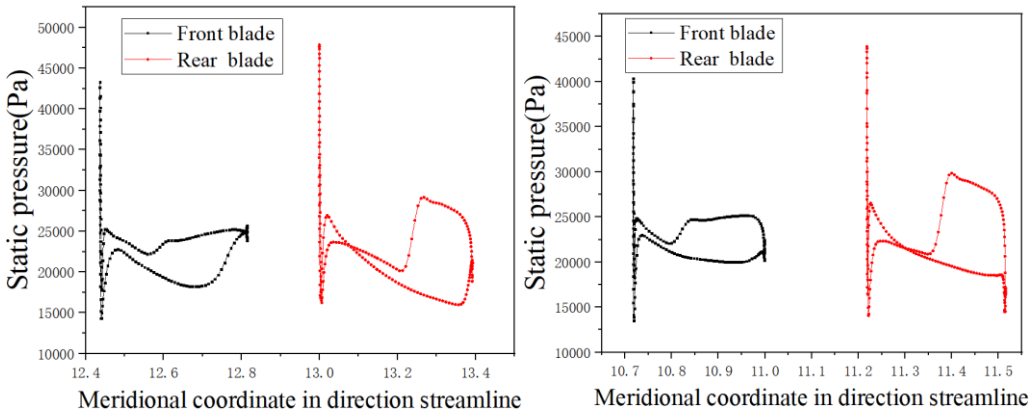

（c）50% blade span (d) 70% blade span

Figure 20 – Static pressure distribution of the contra rotating propeller after optimization

In addition, the power input to the front and rear blades along the blade span is carefully adjusted to reduce flow blockage at the blade roots and shock loss at the blade tips. In the case of the same total thrust, higher propulsion efficiency can be obtained through optimization design.

5. Conclusion

In this paper, a design method of the contra rotating propellers is presented. The design of the contra rotating propellers can reach the designed thrust value. At the same time, the flow characteristics and power distribution of the contra rotating propellers are analyzed, which provides guidance for the aerodynamic design of the contra rotating propellers.

6. Copyright Statement

References

[1] Rohrbach C, Metzger F. The Prop-Fan-A new look in propulsors[C]//*11th Propulsion Conference*. 1975: 1208.

[2] Ji L C, Xiang L, Huang H B, et al. The revelations from the research about the vaneless counter-rotating turbine[J]. *ISABE Paper*, 2003, 1040: 2003.

[3] Backstroem T V , Hobson G , Grossman B , et al. Investigation of the performance of a CFD-designed transonic compressor stage[C]// Aiaa/asme/sae/asee *Joint Propulsion Conference & Exhibit*. 2000.

[4] Wu C H. A general theory of three-dimensional flow in subsonic and supersonic turbomachines of axial-, radial, and mixed-flow types[R]. *National Aeronautics and Space Administration Washington DC*, 1952. (1).

[5] Novak R A , Hearsey R M . A Nearly Three-Dimensional Intrablade Computing System for Turbomachinery[J]. *Journal of Fluids Engineering*, 1977, 99(1):154.

[6] Denton J D , Dawes W N . Computational fluid dynamics for turbomachinery design[J]. *ARCHIVE Proceedings of the Institution of Mechanical Engineers Part C Journal of Mechanical Engineering Science 1*989-1996 (vols 203-210), 1998, 213(2):107-124.

[7] Hager R D. *Advanced turboprop project*[M]. Scientific and Technical Information Division, National Aeronautics and Space Administration, 1988.

[8] Wintucky W T , Stewart W L . Analysis of two-stage counterrotating turbine efficiencies in terms of work and speed requirements[J]. *Technical Report Archive & Image Library*, 1958, 169(3949):931.

[9] Pempie P , Ruet L . Counter-Rotating Turbine Designed for Turbopump Rocket Engine[C]// *Aiaa/asme/sae/asee Joint Propulsion Conference & Exhibit.* 2013.

[10]Siddappaji K , Turner M G , Dey S , et al. Optimization of a 3-Stage Booster: Part 2—The Parametric 3D Blade Geometry Modeling Tool[C]// *Asme Turbo Expo: Turbine Technical Conference & Exposition.* 2011.

[11]University of Cincinnati T-Axi Website http://gtsl.ase.uc.edu/T-AXI/

[12]Turner M G , Merchant A , Bruna D . A Turbomachinery Design Tool for Teaching Design Concepts for Axial-Flow Fans, Compressors, and Turbines[J]. *Journal of Turbomachinery*, 2011, 133(3):937-952.

[13]Turner M , Merchant A , Bruna D . Applications of a Turbomachinery Design Tool for Compressors and Turbines[C]// *43rd AIAA/ASME/SAE/ASEE Joint Propulsion Conference & Exhibit.* 2007.

[14]Bruna D , Cravero C , Turner M G , et al. An Educational Software Suite for Teaching Design Strategies for Multistage Axial Flow Compressors[C]// *Asme Turbo Expo*: Power for Land, Sea, & Air. 2007.

[15]Gutzwiller D P , Turner M G , Downing M J . Educational Software for Blade and Disk Design[C]// *Asme Turbo Expo*: Power for Land, Sea, & Air. 2009.

[16]Goodhand M N , Miller R J . The Impact of Real Geometries on Three-Dimensional Separations in Compressors[J]. *Journal of Turbomachinery*, 2010, 134(2):021007-021007.

[17]Engines G E A. Full Scale Technology Demonstration of a Modern Counterrotating Unducted Fan Engine Concept: Design Report[J]. NASA CR-180867, 1987.

[18]Wennerstrom A J. *Design of highly loaded axial-flow fans and compressors*[M]. 2000.